Journal of Materials and Construction
ISSN 2734-9438
Website: www. jomc.vn

Random laws of kriging method for simulation of characteristic of corroded surface

Nguyen Tan Phat[1], Dao Duy Kien[1*]

[1]Department of Civil Engineering, University of Technology and Education Ho Chi Minh City

KEYWORDS

Corrosion simulation
Geostatistical
Kriging method
Random law
Corrosion distribution

ABSTRACT

The geostatistical method to simulate the corrodded surface of steel structures is one of the most accurate corrosion simulation methods, clearly simulating the correlation of corrosion depth and corrosion characteristics on the steel surface. This study applied geostatistical theory, specifically Kriging, to simulate 11 times based on experimental data. The data set has a length of 200mm, a width of 36mm, and a grid spacing of 1mm. The results of each simulation were compared with those of the specimen data set from the experiment. The Kriging method can not only create a spatial distribution of the corrosion surface with arbitrary length, width, and grid dimensions but also achieve high reliability of characteristic values such as average value, min, max, variance, STDEV, Lag distance, average semivariance, Pairs, Nugget variance (Co), Structural varianceSill (Co + C), Range a, ... as well as the histogram distribution rule. The changing trend of the corrosion surface over time is also accurately predicted. They are creating favorable conditions to determine the behavior of corroded steel structures over time. However, creating a spatial distribution surface by Kriging is still random when each surface simulation is not the same, making the simulation results challenging to apply to finding the first corrosion point in practice.

1. Introduction

In the late 1960s, industrialization began, and the service life of the existing steel structure has almost reached 50 years; it is necessary to establish measures for the stability and long-term service life of the aging, corroded steel structure over time. Severe corrosion damage occurs in steel structures with boundaries or contact with concrete, such as steel structures of bridges, or in large steel oil and gas tanks, concrete roads, shoulder guardrails, steel molds with concrete table tops, and top flange steel accessories of underground works [1, 2].

Corrosion damage to steel parts in contact with concrete by quantitative inspection method is impossible. Therefore, the paint system on steel structures may deteriorate faster than other structural systems. After the paint layer deteriorates, corrosion can occur rapidly on the steel surface. If severe corrosion damage is transferred to the main structural components, eventually, the failure of the main components, leading to the collapse of the structural system, may occur. However, it is difficult to check this corrosion problem when the corroded surface develops because the corrosion is environmentally heterogeneous and is affected by many corrosion factors such as temperature, relative humidity, sea salt in the air, and wet time, unlike other corrosion problems of structural steel [3, 4].

Thus, the harm of corrosion is apparent. Moreover, corrosion becomes the main danger to steel structures. Periodic protection and maintenance of steel structures by painting is the only method to solve the consequences of corrosion. This method only partially solves the problem from the design stage of steel structures. Therefore, it is urgent to accurately analyze the behavior of corroded steel structures and propose design standards for corrosion-resistant steel structures. Therefore, many researchers have researched the corrosion of steel structures using many methods such as natural experiments, laboratory experiments, finite element analysis, and simulation.

Various corrosion models to evaluate and predict corrosion characteristics have been proposed and widely applied to ships, offshore drilling platforms, power and chemical plants, and steel bridges. Paik et al. [5-7] measured the corrosion depth of seawater ballast tanks used on ships for 27 years. They proposed statistical characteristics (i.e., mean, variance, and distribution) of corrosion losses as a function of time. Guedes Soares et al. [8] examined various environmental factors affecting corrosion under seawater immersion conditions. Using field data, they proposed a mathematical model incorporating their effects on corrosion degradation over the ship's life. The application of accelerated cyclic corrosion testing to investigate the corrosion of steel structures is common and has been widely performed. Accordingly, Itoh et al. [9] performed accelerated exposure testing using S6 cycles for uncoated and coated steel plates. They also proposed time-dependent corrosion losses and weight loss and presented the application of accelerated cyclic corrosion testing to evaluate the corrosion resistance of steel bridge components. The shape of the corroded surface of the steel plate was analyzed by statistical methods to understand the influence of the corrosive environment and the damage caused by the increased corrosion [10-13]. Gou et al. [14] applied the Weibull distribution function to represent the probability density function of corrosion depth on loss. Furthermore, they proposed that the Weibull distribution is the most suitable method to represent the

*Corresponding author: kiendd@hcmute.edu.vn
Received 02/03/2025, explanation 08/04/2025, accepted 09/04/2025
Link DOI: https://doi.org/10.54772/jomc.v15i01.855

corrosion characteristics of waste on central storage tanks during the ship's service life.

The fatigue performance of corroded aluminum alloy materials has been widely studied in recent years, but the information on steel structures still needs to be improved. Only a few studies on this issue [15-18] exist. These studies all concluded that corrosion can significantly reduce the fatigue resistance of steel materials. The stress concentration coefficient is one of the essential coefficients that can represent the fatigue state of corroded steel. The influence of stress concentration of corrosion pits with different depths and pit diameters has been studied by [19]. However, experimental methods have obtained many positive results. However, corrosion is a process that takes too much time and money. Therefore, to overcome the limitations of experimental methods, many researchers have proposed finite element methods or simulation models and algorithms to study corrosion. Selecting an appropriate interpolation procedure to predict corrosion is a complex task due to the spatial variability of many corroded surface parameters and environmental factors [20-21]. Many interpolation and approximation methods have been developed to simulate the corrosion of steel structures. These methods include artificial neural networks (ANNs), fuzzy logic methods, and statistical prediction methods [22]. Among them, artificial neural networks are an effective numerical tool inspired by biological neural systems that can be used to perform computational simulations. They can be used to model and describe atmospheric corrosion processes based on experimental observations. Networks can be designed and trained to estimate the corrosion rate of metallic materials from a set of environmental parameters and relevant material data. Accordingly, many researchers have developed corrosion prediction using the ANN method [23].

Inverse Distance Weighting (IDW) is a weighted average interpolation method that can be exact or smooth. With Inverse Distance Weighting, the data is weighted during interpolation so that the influence of one point relative to another decreases with distance from the grid node. Weights are assigned to the data through the use of weighting power, which controls how the weighting coefficients decrease as the distance from the grid node increases. The larger the weighting power, the fewer influence points farther from the grid node will have during interpolation. Typically, the IDW method acts as an exact interpolator, which can be used to predict spatial surfaces [24-25]. Kriging was first introduced by Krige [26]. Kriging is a geographic gridding method that has proven valuable and popular in many fields. This method produces visually appealing maps from irregularly spaced data. Kriging reveals suggested trends in the data; for example, high points may be connected along a ridge rather than isolated by bull's-eye-like contours. Kriging is a very flexible meshing method. Kriging's default values can be accepted to produce an exact data mesh, or Kriging can be customized to a dataset by specifying an appropriate variance model [27-31]. Depending on user-specified parameters, Kriging can be an exact interpolator or a smoothing one. It incorporates anisotropy and underlying trends efficiently and naturally. Therefore, the best simulation method for corrosive surface properties and other fields is estimated using Kriging.

This study focuses on simulating and predicting the characteristics of corrosion surfaces and, at the same time, estimating and predicting the development and change of corrosion surfaces over time by applying geostatistical methods. The geostatistical theory is the most suitable for simulating corrosion over time through the Kriging method. The study has proposed a model and algorithm for the simulation method. The simulation was performed 11 times based on data of 1 corrosion surface obtained from experiments, which means creating 11 corrosion surfaces from simulation. The results of corrosion characteristics of 11 simulations show high accuracy when compared with specimen data. Especially values such as minimum corrosion depth, maximum corrosion depth, average corrosion depth, and corrosion distribution trend on the surface histogram and variogram. However, the results also show the randomness of the data set obtained; the corrosion positions of the 11 times are not the same as the specimen data. This is considered a difficulty and limitation of the method that needs to be improved.

2. Geostatistical theory

2.1. General

Geostatistics is one of the research methods used in geology. Geostatistics analyzes mines' formation, development, and distribution, especially using statistical and mathematical models. Geostatistics is also widely applied in related sciences such as petroleum geology, hydrogeology, hydrology, meteorology, oceanography, geochemistry, ore extraction, geography, forestry, environmental control, landscape ecology, and agriculture. Geostatistics explains not only its applications in geographic information systems but also in applications of numerical mathematical analysis in spatially variable data systems. The digital elevation model (DEM) is the most critical data from which numerical values are extracted. Geostatistics is also applied in other branches of human geography, especially to the spread of disease (epidemiology), business and military planning (logistics), and the development of efficient spatial systems.

The most important issues that geostatistical models address are the dependencies and regularities in distribution.

2.2. Variogram on spatial statistical techniques

a) Spatial Covariance, Correlation and Semivariance

Covariance and correlation are measures of the similarity between two different variables. To extend these measures of spatial similarity, consider a scatterplot where the data pairs represent measurements of the same variable made some distance apart. The separation distance is usually called “lag,” as used in time series analysis [32]. To formalize the definition of these statistics, the definitions for some notation are as follows:

U: vector of spatial coordinates

z(u): variable under consideration as a function of spatial location

h: lag vector representing separation between two spatial locations
z(u+h): lagged version of variable under consideration
N(h) representing the number of pairs separated by lag. we can compute the statistics for lag h as:

Covariance: $C(h) = \frac{1}{N(h)}\sum_{\alpha=1}^{N(h)} z(u_\alpha).z(u_\alpha + h) - m_0.m_{+h}$

Correlation: $\rho(h) = \frac{C(h)}{\sqrt{\sigma_0.\sigma_{+h}}}$

Semivariance: $\gamma(h) = \frac{1}{2N(h)}\sum_{\alpha=1}^{N(h)}[z(u_\alpha + h) - z(u_\alpha)]^2$

where m_0 and m_{+h} are the means of the tail and head values:

$$m_0 = \frac{1}{N(h)}\sum_{\alpha=1}^{N(h)} z(u_\alpha); \quad m_0 = \frac{1}{N(h)}\sum_{\alpha=1}^{N(h)} z(u_\alpha + h)$$

and σ_0 s and σ_{+h} are the corresponding standard deviations:

$$\sigma_0 = \frac{1}{2N(h)}\sum_{\alpha=1}^{N(h)}[z(u_\alpha) - m_0]^2; \quad \sigma_{+h} = \frac{1}{2N(h)}\sum_{\alpha=1}^{N(h)}[z(u_\alpha + h) - m_{+h}]^2$$

b) Semivariogram model

For kriging (or stochastic simulation), we must replace the empirical semivariogram with an acceptable semivariogram model. Part of this is that the kriging algorithm will need access to semivariogram values for lag distances other than those used in the empirical semivariogram. More importantly, the semivariogram models used in the kriging process must obey specific numerical properties for the kriging equations to be solvable. Therefore, statisticians choose from a palette of acceptable or licit semivariogram models.

Using *h* to represent lag distance, *a* to represent (practical) range, and *c* to represent sill, the five most frequently used models are:

Nugget: $g(h) = \begin{cases} 0 \ if \ h = 0 \\ c \ otherwise \end{cases}$

Spherical: $g(h) = \begin{cases} c.\left(1.5\left(\frac{h}{a}\right) - 0.5\left(\frac{h}{a}\right)^3\right) \ if \ h \le 0 \\ c \ otherwise \end{cases}$

Semi-variogram γ(h) is a two-point statistical function, which explain the correlation of the specimen values. The typical semi-variogram model, the relationship between semi-variogram and lag distance is expressed as range and sill.

Sill (γ) or Co: The semivariance value at which the variogram levels off and also used to refer to the "amplitude" of a certain component of the semivariogram.

Range (h): The lag distance at which the semivariogram (or semivariogram component) reaches the sill value. Presumably, autocorrelation is essentially zero beyond the range.

Nugget: In theory the semivariogram value at the origin (0 lag) should be zero. If it is significantly different from zero for lags very close to zero, then this semivariogram value is referred to as the nugget. The nugget represents variability at distances smaller than the typical specimen spacing, including measurement error.

2.3. Kriging method in spatial statistical techniques

This study used ordinary kriging to estimate the 3D corroded steel surface geometry with arbitrarily distributed corrosion depth, as shown in (Figure 1). For ordinary kriging, rather than assuming that the mean is constant over the entire domain, we assume that it is constant in the local neighborhood of each estimation point, that is, that $m(u_\alpha) = m(u_\alpha)$ for each nearby data value, $Z(u_\alpha)$, that we are using to estimate Zu. In this case, the Kriging estimator can be written as:

$$Z^*(u) = m(u) + \sum_{\alpha=1}^{n(u)} \lambda_\alpha(u)[Z(u_\alpha) - m(u)]$$

And also the semivariogram γ(h) is the covariance function of the exponential model was applied in this study.

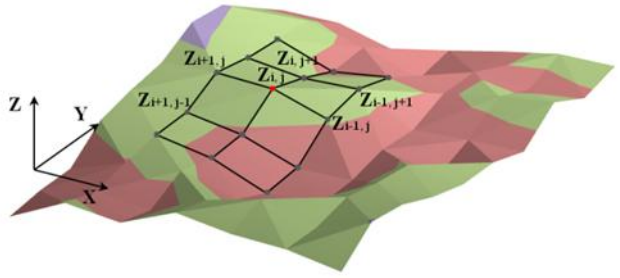

Figure 1. Kriging model for Spatial Data.

3. Corrosion simulation using Kriging method

3.1 Models and algorithms

The summary concept of the time-dependent numerical simulation of 3D corroded surfaces using spatial statistical techniques is shown in the flowchart below:

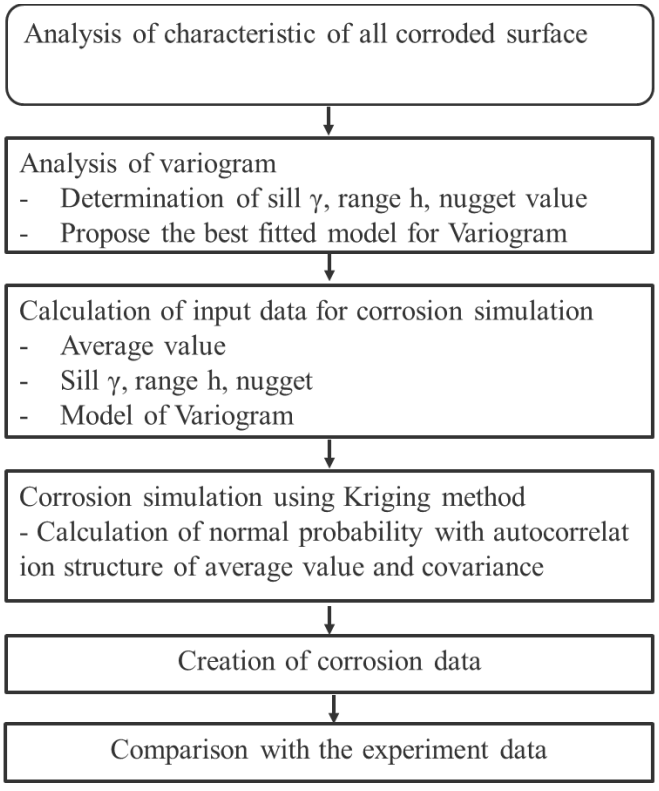

3.2 Data for corrosion simulation

The original data were obtained from the experimental measurement results of corroded steel specimen. After collecting the original data set of the corroded surface, the author used that data set to analyze and simulate corrosion data using the Kriging method through R software.

4. Simulation result and discussion

4.1 Summary of results

The data of 11 simulation datasets were collected and after analyzing the required values, we have the following Table 1.

4.2 Corrosion distribution over the entire surface

The simulation with the most significant corrosion depth is the 6th. The 11 time of simulation has several corrosion areas and is concentrated in the middle. The simulations show more corrosion areas (8/11 times), as shown in (Figure 2). Figure 3 presents a 3D representation of the corrosion distribution on the surface, helping us to see more clearly the locations of the most profound corrosion distribution and the locations of the most concentrated corrosion.

Table 1. Summary table of original and simulation data.

No	Min	Max	Aaverage	Variance	STDEV	Lag distance	Avg Semi-variance	Pairs	Nugget variance (Co)	Structural variance Sill (Co + C)	Range a	Best fit
Refer	0.01	2.03	1.045632648	0.234891078	0.484655628	4.5	0.0687	486266	0.0167	0.2444	21.8	Sph
No.1	-0.592568332	2.391667432	1.061603332	0.220381569	0.469448154	4.5	0.0894	486266	0.0047	0.2234	22.1	Sph
No.2	0.649837672	1.67830354	1.067073091	0.02463582	0.156958021	4.5	0.0665	486266	0.0071	0.1992	20.2	Sph
No.3	-0.358304709	2.459448018	1.079504633	0.195584911	0.442249828	4.5	0.0695	486266	0.0119	0.2048	22.8	Sph
No.4	-0.401318361	2.519687533	1.039826314	0.216155309	0.464925058	4.5	0.076	486266	0.0001	0.2222	18.3	Sph
No.5	-0.646697269	2.52706586	0.994553265	0.26033181	0.510227214	4.5	0.0821	486266	0.0058	0.2736	22.2	Sph
No.6	-0.949908451	3.062354038	1.097527205	0.347254429	0.589282979	4.5	0.0973	486266	0.043	0.36	16.6277	Gaussian
No.7	-0.629976476	2.605613824	0.970712849	0.286897403	0.535628045	4.5	0.0713	486266	0.0001	0.3152	47.1	Exp
No.8	-0.372056631	2.332890152	0.97159058	0.177747962	0.421601663	4.5	0.075	486266	0.0027	0.1814	16.1	Sph
No.9	-0.629976476	2.605613824	0.970712849	0.286897403	0.535628045	4.5	0.0713	486266	0.0001	0.3152	47.1	Exp
No.10	-0.737262509	2.518156704	1.039825455	0.227141411	0.476593549	4.5	0.0749	486266	0.0373	0.2396	18.1865	Gaussian
No.11	0.649837672	1.67830354	1.067073091	0.02463582	0.156958021	4.5	0.0749	486266	0.0373	0.2396	18.1865	Gaussian

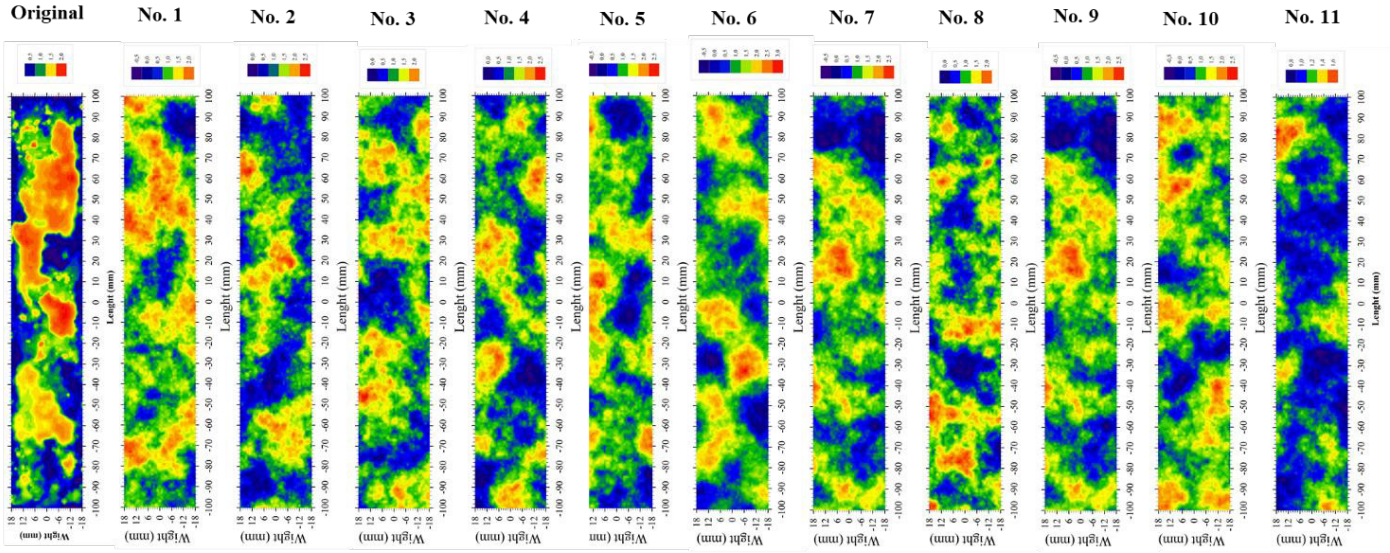

Figure 2. Surface distribution after corrosion shown by contour plot

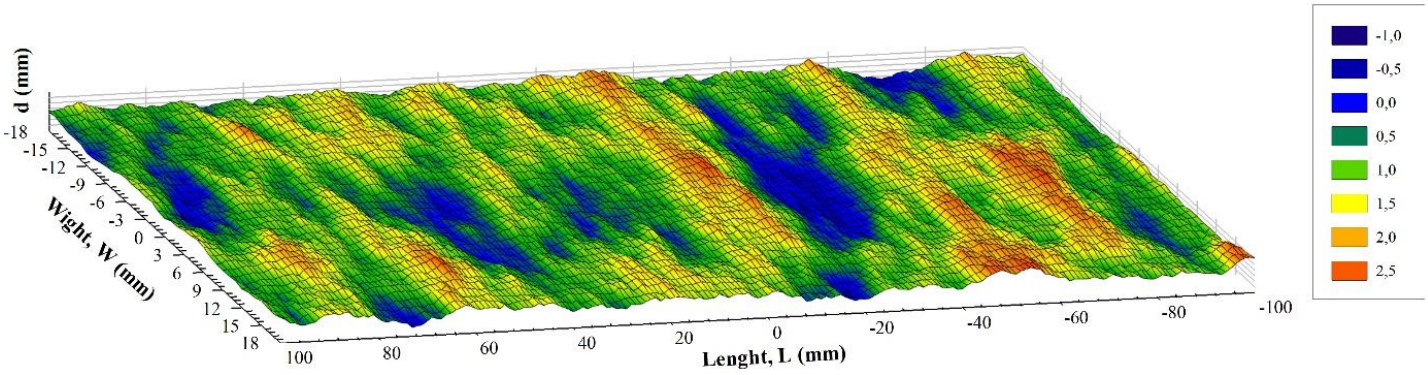

Figure 3. 3D corroded surface of original and simulation data.

4.3 Corrosion distribution on longitudinal section

The corrosion depth in the longitudinal section of the original corrosion data and the corrosion data of 11 simulations tend to be quite similar in shape and depth distribution in the longitudinal section, as shown in (Figure 4).

For the average corrosion depth line of the original data set, there are two edges, which are the two most minor corrosion points and tend to increase corrosion in the middle. Corrosion is regular and periodic and tends to change direction within the same limit amplitude (0.3 to 1.8mm).

The simulation results are pretty random, not in a specific direction:

- Edge: The corrosion coordinates at the two edges do not follow the corrosion law of the actual specimen.
- Middle: The chart trends are pretty similar.
- The number of reversals of the chart belly is close to each other. The belly tends to be similar, but there will be differences in value.

4.4 Analysis of simulation randomness

The charts and (Table 1) show that the error area of the Variogram values of the original corrosion data values has a significant difference compared to the corrosion data values of 11 simulations. The Variance, STDEV, Nugget variance (Co), Structural variance Sill (Co + C), and Range values significantly differ in error values ranging from 26.15% to 116.06%. However, the R2 value has a small error.

4.4.1. Location of maximum corrosion depth

Figure 5 shows that most of the deepest corrosion locations tend to be concentrated on the right side of the specimen, concentrated thickly with up to 6 times the deepest corrosion location appearing in the area (40-100 mm) in the x direction - the specimen length direction. According to the y-direction - Horizontal direction of the specimen, the most significant corrosion locations appear most often on the left side, appearing eight times and concentrated in the area (-5 to -20 mm).

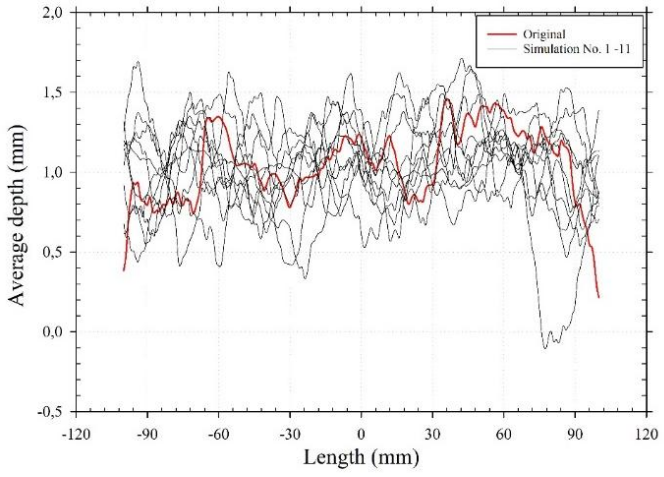

Figure 4. Comparison of average depth on longitudinal section of specimen.

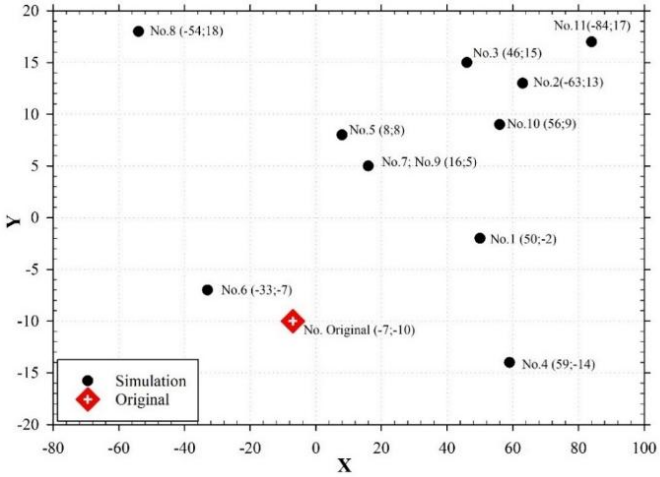

Figure 5. Comparison of random occurrence of points with maximum corrosion depth.

4.4.2. Comparison of randomness of values between simulated and experimental data sets

4.4.2.1. Average value of corrosion depth

Figure 6 shows that the percentage error of the average corrosion depth between 11 simulations is similar to the average, controlled in the 4.76 - 7.62% range. It shows that the corrosion simulation data gives almost accurate corrosion depth results.

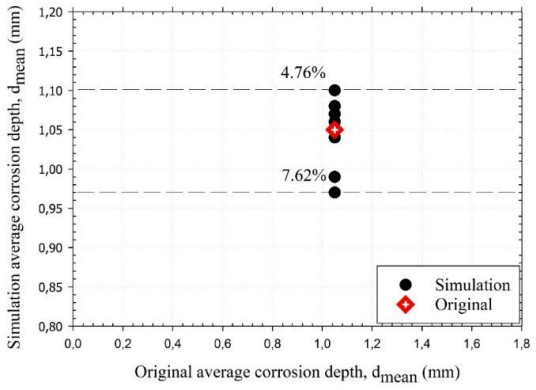

Figure 6. Comparison of randomness of average corrosion depth values.

4.4.2.2. Maximum value of corrosion depth

Figure 7 shows that the percentage of error of the maximum corrosion depth value of 11 simulations differs quite a lot from the actual maximum corrosion depth value; one random simulation differs by 50.74% from the original data. However, most simulations will have a maximum corrosion depth with less error, mainly about 25-30%. It shows that the corrosion simulation data gives the maximum corrosion depth value, which needs to be revised.

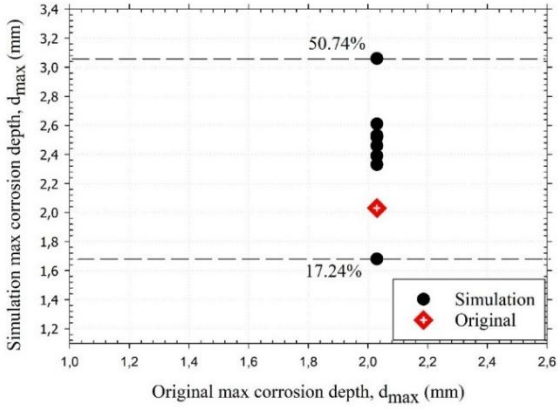

Figure 7. Comparison of randomness of maximum corrosion depth values.

4.4.2.3. Minimum value of corrosion depth

Figure 8 shows that the error percentage of the smallest corrosion depth value of 11 simulations differs significantly from the smallest corrosion depth value, with the highest error being 9600%. The corrosion simulation data shows almost inaccurate results for the most minor corrosion depth.

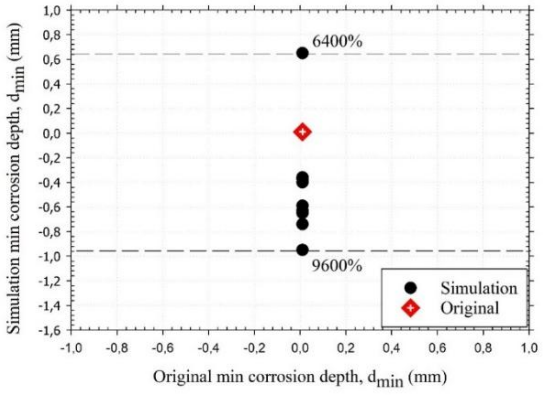

Figure 8. Comparison of randomness of minimum corrosion depth values.

5. Variogram values of corrosion depth

Figure 9 indicated that the variogram values tend to change around the original data. Based on these simulated data, the Kriging simulation method will produce the data sets that vary by a certain amount from the original data.

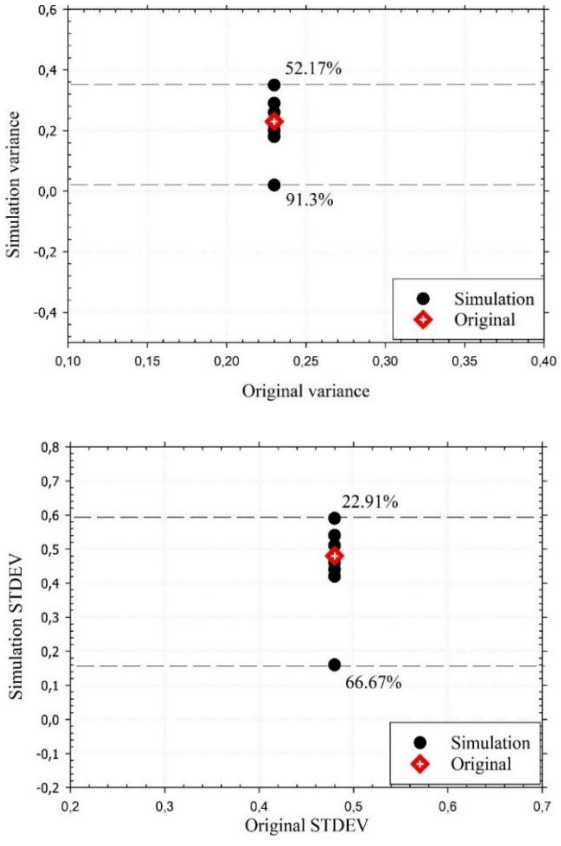

Original Variance STDEV

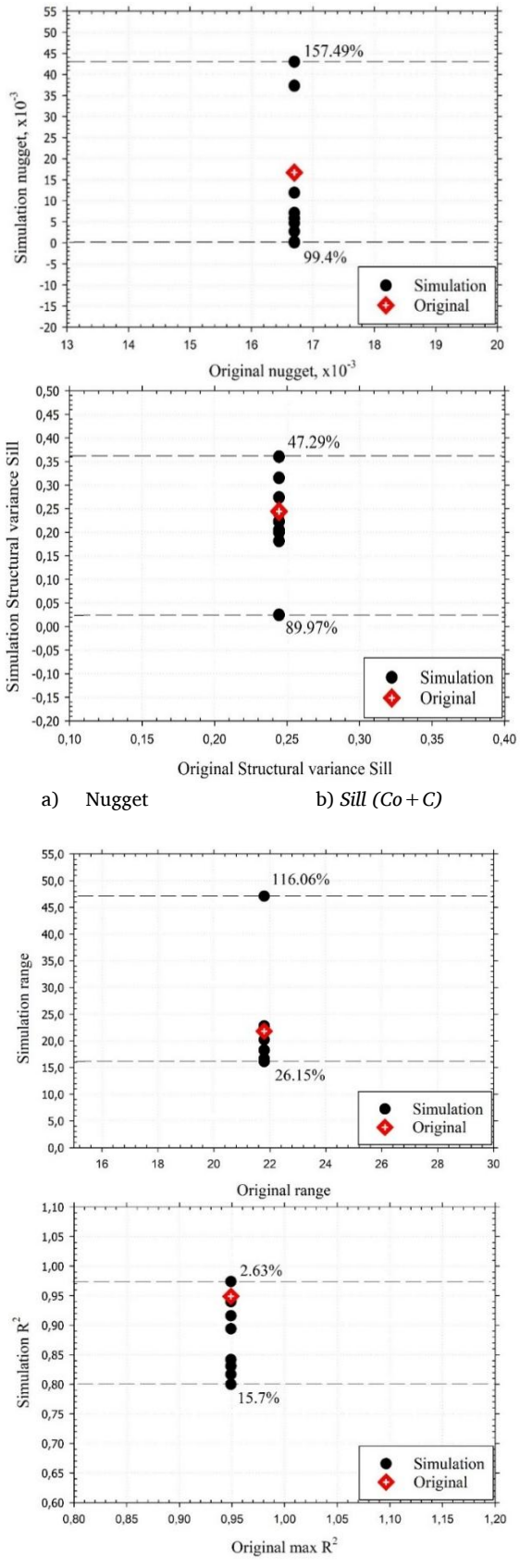

a) Nugget b) *Sill (Co + C)*

Range a d) giá trị R

Figure 9. Comparison of randomness of variogram values.

Table 2. Errors between original and simulated corrosion data.

Value	Error between original and simulated corrosion	
	Min	Max
Variance	52.17%	91.30%
STDEV	22.91%	66.67%
Nugget variance (Co)	99.40%	157.49%
Structural variance Sill (Co + C)	47.29%	89.97%
Range a	26.15%	116.06%
R^2	2.63%	15.70%

5. Conclusion

The 3D corrosion surface shape of the steel plate simulated 11 times by spatial statistical theory was compared with the estimated surface of the experimental steel plate. The results showed that:

- The Kriging method model is quite suitable for simulating the description of the spatial distribution of the corrosion surface. However, the corrosion distribution area with the most incredible depth tends to concentrate on the right side of the specimen in the X direction (specimen length direction) and the left side of the specimen in the Y direction (specimen width direction). It proves that the Kriging method produces a hybrid data set that produces similar corrosion surfaces.
- It is found that the distribution of the point with the maximum corrosion depth (the point that is most likely to cause structural damage on the steel plate) is entirely random. But we can see the trend of the deepest corrosion points distributed on the left side of the steel specimen in the width direction,
- The maximum value, average, Variance value, and STDEV of corrosion depth have insignificant differences between the original data and the simulation. However, the Range of Structural variance Sill (Co + C) and Nugget variance (Co) differ significantly. So, the Kriging algorithm to simulate corrosion still has some factors that are not optimal, and the algorithm needs to be improved.
- From that, it shows that the randomness of the corrosion data set from the simulation using the spatial geostatistics method is still a big challenge with no regularity.

Acknowledgments

This work belongs to the project grant No: T2024-01HVCH. funded by Ho Chi Minh City University of Technology and Education, Vietnam.

References

[1] U.R. Evans, (1966), "The Corrosion and Oxidation of Metals: Scientific Principles and Practical Applications", *Edward Arnold Publishers Ltd., London, 1966.*

[2] N.D. Tomashev, (1966), "Theory of Corrosion and Protection of Metals", *The MacMillan Co., New York,* 1966.

[3] Jeom Kee Paik, Anil K. Thayamballi, Young Il Park, Joon Sung Hwang, (2003), "A time-dependent corrosion wastage model for seawater ballast tank structures of ships", *Corrosion Science*, Vol. 46, pp. 471-486.

[4] Jeom Kee Paik, Jae Myung Lee, Young II Park, Joon Sung Hwang, Chang Wook Kim, (2003), "Time-variant ultimate longitudinal strength of corroded bulk carriers", *Marine Structures*, Vol. 16, pp. 567–600.

[5] Jeom Kee Paik, Jae Myung Lee, Joon Sung Hwang, Young Il Park, (2003), "A Time-Dependent Corrosion Wastage Model for the Structures of Single- and Double-Hull Tankers and FSOs and FPSOs", *Marine Technology*, Vol. 40 (3), pp. 201–217

[6] Yoshito Itoh, In-Tae Kim, (2006),"Accelerated cyclic corrosion testing of structural steels and its application to assess steel bridge coatings", *Anti-Corrosion Methods and Materials*, Vol. 53 (6), pp. 374 – 381.

[7] P. Montoya, I. Díaz., N. Granizo, D. de la Fuente, M. Morcillo, (2013), "An study on accelerated corrosion testing of weathering Steel", *Materials Chemistry and Physics,* Vol. 142, pp. 220 – 228

[8] Daisuke Mizuno, Katsuya Hoshino, Shinji Otsuka, Sakae Fujita, Nobuyoshi Hara, (2014), "An Appropriate Specimen Configuration for Evaluating the Perforation Corrosion Resistance of Automotive Coated Steel Sheets in Accelerated Corrosion Tests", *Corrosion Science,* Vol. 71(1), pp. 92-100.

[9] R.E. Melchers, M. Ahammed, R. Jeffrey, G. Simundic, (2010), "Statistical characterization of surfaces of corroded steel plates", *Marine Structures*, Vol. 23, pp. 274–287.

[10] Jinting Guo, Ge Wang, Lyuben Ivanov, Anastassios N. Perakis, (2008). "Time-varying ultimate strength of aging tanker deck plate considering corrosion effect", *Marine Structures*, Vol. 21, pp. 402–419.

[11] Matsukura. T, Kawamura. Y, Khoo. E, (2011). "A study on long-term prediction of corrosion wastage". *In Advances in Marine Structures - Proceedings of the 3rd International Conference on Marine Structures, MARSTRUCT, pp.* 699-705

[12] J. W. van de Lindt, S. Pei, (2006), "Buckling Reliability of Deteriorating Steel Beam Ends", *Electronic Journal of Structural Engineering,* Vol. 6.

[13] Shigenobu Kainuma, Naofumi Hosomi, (2008), "Fatigue life evaluation of corroded structural steel members in boundary with concrete", *International Journal of Fracture*, Vol. 157, pp. 149-158.

[14] M. A. Stephens, (1974), "EDF Statistic for good of fit and some comparisons", *Journal of American statistical Association,* Vol. 69, pp. 730-737.

[15] K.F. Khaled, Abdelmounam Sherik, (2013), "Using Neural Networks for Corrosion Inhibition Efficiency Prediction during Corrosion of Steel in Chloride Solutions", *Int. J. Electrochem*, Vol. 8, pp. 9918 – 9935.

[16] Mazura Mat Din, Norafida Ithnin, Azlan Md. Zain, Norhazilan Md Noor, Maheyzah Md Siraj, Rosilawati Md. Rasol, (2015), "An Artificial Neural Network Modeling For Pipeline Corrosion Growth Prediction", *ARPN Journal of Engineering and Applied Sciences,* Vol. 10(2), pp. 512-519.

[17] R.A. Cottis, Li Qing, G. Owen, S.J. Gartland, I.A. Helliwell, M. Turega, (1999), "Neural network methods for corrosion data reduction", *Materials and Design*, Vol. 20, pp. 169-178.

[18] Joerg Panzer NEXO, Daniele Ponteggia Audiomatica, (2011), "Inverse Distance Weighting for Extrapolating Balloon-Directivity-Plots", *The AES 131th Convention*, New York, pp. 1-8.

[19] Yanjun Zhang, Cuiling Xian, Huajin Chen, Michael L. Grieneise, Jiaming Liu, Minghua Zhang, (2016), "Spatial interpolation of river channel topography using the shortest temporal distance", *Journal of Hydrology*, Vol. 542, pp. 450–462.

[20] D. G. Krige, (1951), "A statistical approach to some basic mine valuation problems on the Witwatersrand", *Journal of the Chemical, Metallurgical and Mining Society of South Africa*, Vol. 52, pp. 119-139.

[21] J.C. Walton, G. Cragnolino, S.k. Kalandros, (1996), "A numerical model of crevice corrosion for passive and active metals", *Corrosion Science*, Vol. 38, No. 1, pp. 1-16.

[22] Rodolfo M. Mendes, Reinaldo Lorandi, (2008), "Analysis of spatial variability of SPT penetration resistance in collapsible soils considering water table depth", *Engineering Geology,* Vol. 101, pp. 218 –225.

[23] ASTM Designation: D6899-03. "Standard Guide for Laboratory Cyclic Corrosion Testing of Automotive Painted Steel". 2003

[24] M. A. Stephens, (1974), "EDF Statistic for good of fit and some comparisons", *Journal of American statistical Association,* Vol. 69, pp. 730-737.

[25] *Papoulis, Athanasios Papoulis. Pillai, S. Unnikrishna, (2002), "Probability, Random Variables, and Stochastic Processes (4th ed.)", Boston: McGraw-Hill. ISBN 0-07-366011-6.*

[26] Japanese Standards Association (1992), "Anticorrosive Paint for general use", JIS K5621.

[27] Guoqiang Zhang, B. Eddy Patuwo, Michael Y. Hu, (1997), "Forecasting with artificial neural networks: The state of the art", *International Journal of Forecasting* , Vol. 14, pp. 35–62

[28] Elaine D. Kenny, Ramón S.C. Paredes, Luiz A. de Lacerda, Yuri C. Sica, Gabriel P. de Souza, José Lázaris, (2009), "Artificial neural network corrosion modeling for metals in an equatorial climate", *Corrosion Science*, Vol. 51, pp. 2266–2278.

[29] Mazura Mat Din, Norafida Ithnin, Azlan Md. Zain, Norhazilan Md Noor, Maheyzah Md Siraj, Rosilawati Md. Rasol, (2015), "An Artificial Neural Network Modeling For Pipeline Corrosion Growth Prediction", *ARPN Journal of Engineering and Applied Sciences,* Vol. 10(2), pp. 512-519.

[30] O. Oluwole, N. Idusuyi, (2012), "Artificial Neural Network Modeling for Al- Zn- Sn Sacrificial Anode protection of Low Carbon Steel in Saline Media", *American Journal of Materials Science*, Vol. 2(3), pp. 62-65.

[31] Eulogio Pardo-Iguzquiza, Mario Chica-Olmo, (2008), "Geostatistics with the Matern semivariogram model: A library of computer programs for inference, kriging and simulation", *Computers & GeoscienceS,* Vol. 34, pp. 1073 –1079.

[32] Carol A. Gotway, Richard B. Ferguson, Gary W. Hergert, Todd A. Peterson, (1996), "Comparison of Kriging and Inverse-Distance Methods for Mapping Soil Parameters", *Soil Sci. Soc. Am. J.*, Vol. 60, pp. 1237-1247.